PAPER

Check for updates

Fluorometric enhancement of the detection of H₂O₂ using different organic substrates and a peroxidase-mimicking polyoxometalate†

Rui Tian,[a] Boyu Zhang,[a] Mingming Zhao,[a] Hangjin Zou,[a] Chuhan Zhang,[a] Yanfei Qi (ID) *[a] and Qiang Ma (ID) *[b]

Simple, sensitive and stable fluorometric sensors based on the polyoxotungstate intrinsic peroxidase ($Na_{10}[\alpha\text{-}SiW_9O_{34}]$) induced fluorescent enhancement of benzoic acid (BA), thiamine (TH) and 3-(4-hydroxyphenyl)propionic acid (HPPA) for the detection of hydrogen peroxide (H_2O_2) are developed for the first time. In three assays, the three non-fluorescent substrates BA, TH and HPPA were oxidized with the ·OH radicals decomposed from H_2O_2 under the catalysis of $Na_{10}[\alpha\text{-}SiW_9O_{34}]$ under basic pH conditions. The optimal conditions for the detection of H_2O_2 were evaluated and possible mechanisms are also discussed. The fluorescence intensity increases were linearly related to the concentration of H_2O_2 in the ranges 1×10^{-8} to 1.6×10^{-6}, 1.6×10^{-6} to 1×10^{-4}, and 1×10^{-5} to 2.5×10^{-4} M with BA, TH, and HPPA as substrates, respectively. Detection limits for the three systems were found to be 6.7×10^{-9}, 2.2×10^{-7} and 9.6×10^{-6} M (3σ), respectively. The RSD values ranged from 2.57% to 4.66%, 0.82% to 4.06%, and 1.08% to 2.75%, respectively. The rates of recoveries were between 99.73% and 113.06%, 95.20% and 104.22%, and 95.28% and 128.76%, respectively. Moreover, the effects of interference were studied. The proposed work was successfully applied to the determination of H_2O_2 in water and a sensitive, rapid and easy to operate assay was built, which has great potential applications in environmental science.

1. Introduction

Hydrogen peroxide exists widely in biological systems, food production, and pharmaceutical, industrial and environmental applications.[1–3] It is a natural product in oxidative metabolic processes in biology, being harmful to organisms when the concentration of H_2O_2 reaches 0.5 mmol L^{-1}.[4] It is also a source of toxic oxygen that produces ·OH radicals,[5] which can lead to disease and senescence in a body. Therefore, the trace determination of H_2O_2 is very important in environmental analysis, biochemical analysis and clinical diagnostics. In recent years, various methods for the determination of H_2O_2 have been developed, such as fluorometry,[6] spectrophotometry,[7,8] chemiluminescence,[9] liquid chromatography[10] and electrochemistry.[11,12] Among these methods, the horseradish peroxidase (HRP)-catalyzed reaction is the most widely used enzymatic reaction.[13] The characteristics of the enzyme have been systematically studied with H_2O_2 as an oxidizing agent and in

the presence of various substances as fluorogenic substrates.[4] Although HRP has high specificity and sensitivity, its instability and high cost restrict its application.[14] Compared to HRP, artificial enzyme mimics are more economic due to their high thermal stability, high tolerance of practical conditions, good adaptability to abiotic/biotic reactions and low cost of preparation and purification.

The development of artificial enzyme mimics as well as their expanding applications in various fields, such as pharmaceuticals, fine-chemical syntheses, chemical and biological sensing, and proteome analyses, have been actively pursued for decades.[15] To date, a large number of artificial enzymes have been explored to mimic the structures and functions of naturally occurring enzymes including cyclodextrins, metal complexes, porphyrins, polymers, dendrimers, biomolecules and nanomaterials.[16–28] Among these, polyoxometalates have aroused special attention due to their mimicking enzyme activity towards peroxidase substrates. Polyoxometalates (POMs) are a large family of inorganic metal-oxide cluster compounds with many remarkable physical and chemical properties and biological activities.[29,30] In particular, POMs undergo a fast and reversible multi-electron redox process without any significant structural changes, that makes them useful as redox sensors. Based on the outstanding properties of POMs, POMs and their hybrids have been utilized in

[a]*School of Public Health, Jilin University, Changchun, Jilin 130021, China. E-mail: qiyanfei@jlu.edu.cn; Tel: +86-431-85619441*

[b]*Department of Analytical Chemistry, College of Chemistry, Jilin University, Changchun 130012, China. E-mail: qma@jlu.edu.cn*

a colorimetric assay of HepG2 cells, H_2O_2 and glucose.[31–38] However, by far the majority of POMs with intrinsic peroxidase-like activity are stable under acid aqueous conditions. While the complex practical conditions for H_2O_2 detection require high temperature and alkalinity (20–98 °C, pH $\geq$ 7),[7,10] which hamper the applications of POMs. In a recent paper, we first reported the fluorescent quenching of CdTe quantum dots for the measurement of H_2O_2 with catalysis by $Na_{10}[\alpha\text{-}SiW_9O_{34}]$ under basic pH aqueous conditions.[39] Considering the HPR enzyme-mimicking properties of $Na_{10}[\alpha\text{-}SiW_9O_{34}]$, new fluorometric methods based on it for the detection of H_2O_2 and several flu-orogenic substrates under alkaline conditions can subsequently be developed. Additionally, more research is needed into the effects of the POM enzyme-mimicking reaction for biological and chemical analysis.

From a combination of the above reasons, herein we design for the first time new fluorometric enhancement methods that explore the catalytic effect of $Na_{10}[\alpha\text{-}SiW_9O_{34}]$ to convert weakly fluorescent substrates into strongly fluorescent substrates in the presence of H_2O_2. Benzoic acid (BA),[13] thiamine (TH)[40] and 3-(4-hydroxyphenyl)propionic acid (HPPA)[41] have been employed as fluorogenic substrates for hydrogen peroxide detection *via* the formation of fluorescent products. In this fluorometric assay, different analytical parameters, such as concentration of substrates and $Na_{10}[\alpha\text{-}SiW_9O_{34}]$, buffer pH, and reaction time were optimized. The catalysis activities and kinetic mechanics of $Na_{10}[\alpha\text{-}SiW_9O_{34}]$ were investigated upon the reaction of hydrogen peroxide with its oxidized substrates, BA, TH and HPPA. Under the optimal reaction conditions, the detection system of BA–$Na_{10}[\alpha\text{-}SiW_9O_{34}]$–$H_2O_2$ shows the most sensitive response to H_2O_2 over the other two systems. The present assays have been successfully applied to the determi-nation of H_2O_2 in water.

2. Experimental section

2.1. Reagents and chemicals

All the chemicals used were of analytical grade without further purification. Benzoic acid (BA), thiamine (TH), 3-(4-hydrox-yphenyl)propionic acid (HPPA) and $Na_2WO_4 \cdot 2H_2O$ were ob-tained from the Guoyao Chemical Research Institute (Shenyang, China). Na_2SiO_3 was obtained from Sinopharm Chemical Reagent Co., Ltd. (Shanghai, China). Na_3PO_4, NaH_2PO_4, NaCl, HCl, Na_2CO_3 and hydrogen peroxide (H_2O_2, 30%) were purchased from Beijing Chemical Works (Beijing, China). The water used in the experiments was purified. The ρ of the water was 18 MΩ cm.

2.2. Instrumentation

The fluorescence measurements were performed on a Shi-madzu RF-5301 PC fluorescence spectrofluorophotometer (Kyoto, Japan). A 1 cm path length quartz cuvette was used in the experiment. The widths of the excitation and emission slits were set to 5.0 and 5.0 nm, respectively. The Fourier Transform Infrared (FTIR) spectrum was recorded in the range 400–4000 cm^{-1} on KBr (FTIR IRAffinity-1s, Shimadzu, Japan). The

pH measurements were performed by a PHS-25 pH meter (Shanghai INESA Scientific Instrument Co. Ltd, China). The purified water was obtained from a SMART-N Heal Force Water Purification System (Shanghai Canrex Analytic Instrument Co., Ltd, Pudong Shanghai China).

2.3. Synthesis of $Na_{10}[\alpha\text{-}SiW_9O_{34}]$

$Na_{10}[\alpha\text{-}SiW_9O_{34}]$ was prepared according to the literature method.[42] Briefly, 0.133 mol of $Na_2WO_4 \cdot 2H_2O$ and 12.5 mmol of Na_2SiO_3 were dissolved in 200 mL of distilled hot water, and then HCl (6 M, 32.5 mL) was slowly added to the above solution with vigorous stirring for 30 min. The mixture was boiled to a volume of 75 mL and then the filtrate was collected. Then, 3.2 mol of Na_2CO_3 solution was slowly added into the filtrate under stirring. The precipitate was collected after 1 h. The solid was stirred with 250 mL of 4 M NaCl and dried under vacuum. The characteristic peaks of $Na_{10}[\alpha\text{-}SiW_9O_{34}]$ (KBr pellet, cm^{-1}) were 987, 936, 869, 836, 705, 655 (Fig. S1†), which are nearly consistent with the values reported in the literature.

2.4. H_2O_2 detection

100 μL of different substrates (the concentrations of BA, TH, and HPPA were 5, 20, and 80 mmol L^{-1}, respectively), 100 μL of 8 mmol L^{-1} $Na_{10}[\alpha\text{-}SiW_9O_{34}]$, 750 μL of 20 mmol L^{-1} phosphate buffer solution (pH = 11.0) were mixed at room temperature. 50 μL of various concentrations of H_2O_2 were added into the mixture, sequentially. After the addition of H_2O_2, the fluores-cence values of the above solutions were measured by a fluo-rescence spectrophotometer (BA: λ_{ex} = 295 nm, λ_{em} = 405 nm. TH: λ_{ex} = 375 nm, λ_{em} = 440 nm. HPPA: λ_{ex} = 330 nm, λ_{em} = 416 nm). The process of H_2O_2 addition to BA, TH and HPPA with $Na_{10}[\alpha\text{-}SiW_9O_{34}]$ as catalyst is shown in Scheme 1.

3. Results and discussion

3.1. The peroxidase-like activity of the $Na_{10}[\alpha\text{-}SiW_9O_{34}]$

The peroxidase-like activity of $Na_{10}[\alpha\text{-}SiW_9O_{34}]$ was verified by fluorometric experiments using BA, TH and HPPA as the substrates. $Na_{10}[\alpha\text{-}SiW_9O_{34}]$ catalyzed the conversion of weakly fluorescent BA to produce fluorescent adduct hydroxylated benzoic acid (OHBA) in the presence of H_2O_2, which showed strong fluorescence at 405 nm when excited at 295 nm. As shown in Fig. 1A, when $Na_{10}[\alpha\text{-}SiW_9O_{34}]$ was added into the BA–H_2O_2 solution, a strong fluorescence peak was obtained. However, there were no strong fluorescence peaks when the solution did not contain H_2O_2 and/or $Na_{10}[\alpha\text{-}SiW_9O_{34}]$, which confirmed that the reaction between BA and H_2O_2 could be catalyzed by $Na_{10}[\alpha\text{-}SiW_9O_{34}]$. Thiamine is a non-fluorescent substrate, but thiochrome, the oxidation product of thiamine with H_2O_2, is strongly fluorescent, showing an excitation maximum at 375 nm and a fluorescence emission maximum at 440 nm. The fluorescence spectrum of the TH–$Na_{10}[\alpha\text{-}SiW_9O_{34}]$–$H_2O_2$ system is shown in Fig. 1B. In comparison, no fluores-cence peaks were observed in the TH, TH–$Na_{10}[\alpha\text{-}SiW_9O_{34}]$ or TH–H_2O_2 systems, which confirmed that the reaction between TH and H_2O_2 could also be catalyzed by $Na_{10}[\alpha\text{-}SiW_9O_{34}]$. HPPA
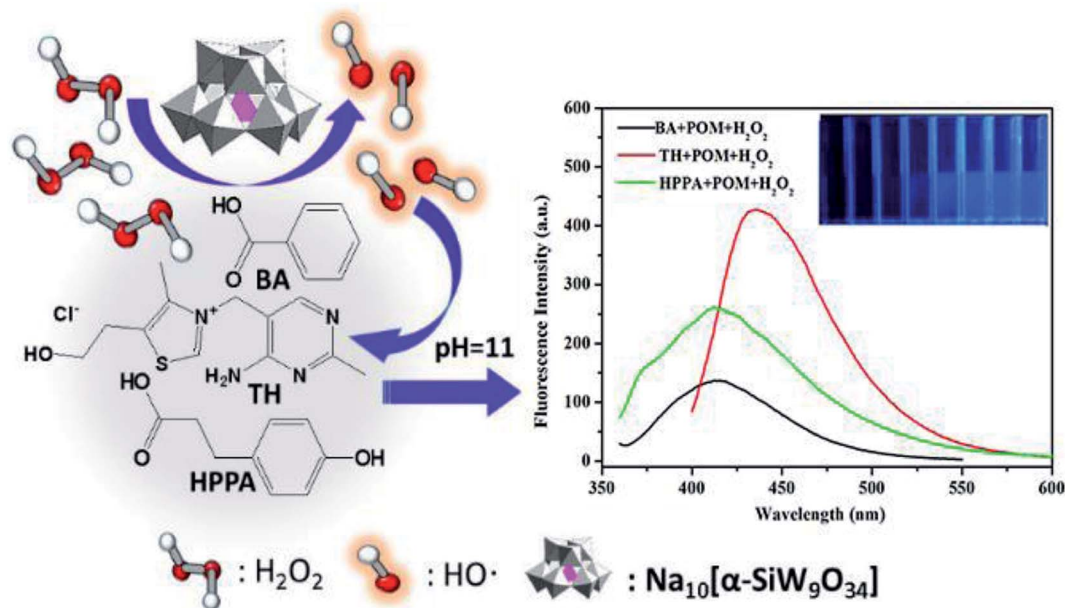
Scheme 1 A schematic illustration of the processes of H_2O_2 addition to BA, TH and HPPA with $Na_{10}[\alpha\text{-}SiW_9O_{34}]$ as catalyst.

is one of the most efficient substrates for evaluating peroxidase activity.[43] More specifically, non-fluorescent HPPA can be oxidized by hydrogen peroxide to yield a strong fluorescent dimer *via* peroxidase catalysis. Following the addition of $Na_{10}[\alpha\text{-}SiW_9O_{34}]$ to the HPPA–H_2O_2 system, a strong fluorescence peak was observed, as shown in Fig. 1C. Like the BA and TH systems, no fluorescence peaks were observed in the HPPA, HPPA–$Na_{10}[\alpha\text{-}SiW_9O_{34}]$ and HPPA–H_2O_2 systems, which indicated that the reaction between HPPA and H_2O_2 could be catalyzed by $Na_{10}[\alpha\text{-}SiW_9O_{34}]$.

3.2. Condition optimization

In order to optimize the possible analytical methods for H_2O_2 determination, the effects of experimental conditions, including reaction time, solution pH, the concentration of substrates, and the concentration of $Na_{10}[\alpha\text{-}SiW_9O_{34}]$ were investigated.

3.2.1. Effect of reaction time. As shown in Fig. 2A, the fluorescence intensity of the generated OHBA rapidly increases with reaction time initially, and then tends towards saturation after 600 s, which indicates that the added H_2O_2 is completely consumed by oxidation of the substrate BA. Thus, 10 min was chosen as the optimal reaction time. Fig. 2B shows that the fluorescence intensity of the generated thiochrome changed from 0 to 600 seconds, and then tended towards to a constant after 600 s, indicating that the TH–$Na_{10}[\alpha\text{-}SiW_9O_{34}]$–$H_2O_2$ solution was stable during this period. Fig. 2C shows the effects of reaction time (0–900 seconds) on the fluorescence intensity of HPPA–$Na_{10}[\alpha\text{-}SiW_9O_{34}]$ in the presence of H_2O_2. When H_2O_2 was added into an HPPA–$Na_{10}[\alpha\text{-}SiW_9O_{34}]$ aqueous solution, the fluorescence intensity rapidly increased from 0 to 60 seconds, and then tended towards saturation after 600 s, which indicated that the added H_2O_2 was completely consumed by oxidation of the substrate HPPA. Thus, 10 min was chosen as the optimal reaction time in the three different substrate systems.
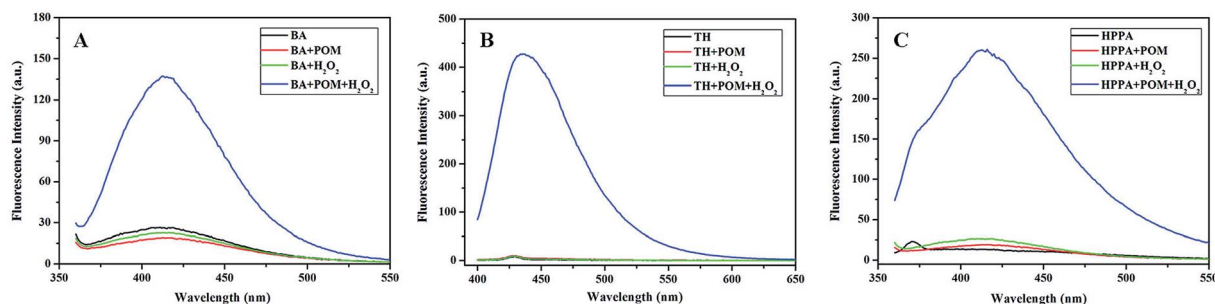

Fig. 1 Fluorescence spectra of the (A) BA–$Na_{10}[\alpha\text{-}SiW_9O_{34}]$–$H_2O_2$ system, (B) TH–$Na_{10}[\alpha\text{-}SiW_9O_{34}]$–$H_2O_2$ system and (C) HPPA–$Na_{10}[\alpha\text{-}SiW_9O_{34}]$–$H_2O_2$ system. Reaction conditions: 8 mmol L^{-1} $Na_{10}[\alpha\text{-}SiW_9O_{34}]$; 100 mmol L^{-1} H_2O_2; 5 mmol L^{-1} BA; 20 mmol L^{-1} TH; 80 mmol L^{-1} HPPA; pH, 11.0; temperature, 25 °C; incubation time, 10 min.
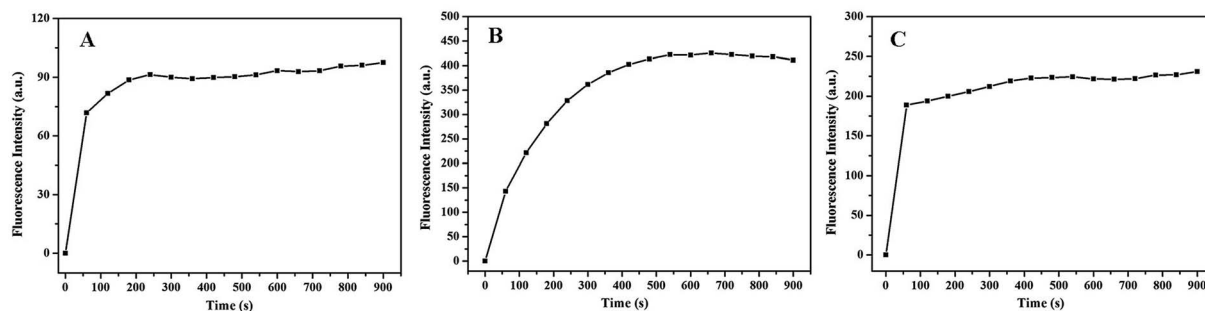
Fig. 2 The effects of reaction time on the fluorescence intensities of the (A) BA–Na$_{10}$[α-SiW$_9$O$_{34}$] system, (B) TH–Na$_{10}$[α-SiW$_9$O$_{34}$] system and (C) HPPA–Na$_{10}$[α-SiW$_9$O$_{34}$] system in the presence of H$_2$O$_2$. Reaction conditions: 8 mmol L^{-1} Na$_{10}$[α-SiW$_9$O$_{34}$]; 100 mmol L^{-1} H$_2$O$_2$; 5 mmol L^{-1} BA; 80 mmol L^{-1} HPPA; pH, 11.0; temperature, 25 °C.

3.2.2. Effect of pH. The solution pH is an important factor affecting catalytic efficiency. To investigate the influence of pH on the different substrate–Na$_{10}$[α-SiW$_9$O$_{34}$]–H$_2$O$_2$ systems, the fluorescence intensities were examined in buffer solutions with various pH values (5.0–11.0). As shown in Fig. 3, the fluorescence intensities of different substrate–Na$_{10}$[α-SiW$_9$O$_{34}$]–H$_2$O$_2$ systems were much faster in basic solutions than in neutral or acidic solutions. Moreover, the BA–Na$_{10}$[α-SiW$_9$O$_{34}$]–H$_2$O$_2$ system, TH–Na$_{10}$[α-SiW$_9$O$_{34}$]–H$_2$O$_2$ system and HPPA–Na$_{10}$[α-SiW$_9$O$_{34}$]–H$_2$O$_2$ system reached their maximum fluorescence intensities when the pH value was 11.0. Therefore, pH 11.0 was selected to be the optimal pH in the different substrate–Na$_{10}$[α-SiW$_9$O$_{34}$]–H$_2$O$_2$ systems.

3.2.3. Effect of different substrate concentrations. To maximize the activity of Na$_{10}$[α-SiW$_9$O$_{34}$], the effects of varying concentrations of the substrates were also investigated. Fig. 4A and D show the influence of BA concentrations on the

fluorescence intensity of the reaction solution. For a given concentration of H$_2$O$_2$ (100 mmol L^{-1}), the fluorescence intensity was enhanced with an increase in the BA concentration up to 5 mM, and then slowly increased beyond 5 mM of BA. Hence, 5 mM BA was selected as the optimal concentration. As shown in Fig. 4B and E, the relationship between the fluorescence intensity of the product and the concentration of TH was investigated between 0.3125 and 50 mM. When the concentration of TH reached 20 mM, the fluorescence intensity of the TH–Na$_{10}$[α-SiW$_9$O$_{34}$]–H$_2$O$_2$ system reached its maximum. Thus, 20 mM TH was selected as the optimal concentration. As shown in Fig. 4C and F, the fluorescence intensity of the reaction system was enhanced as the concentration of HPPA increased to 80 mM, after which it decreased. Thus, 80 mM HPPA was selected as the optimal concentration.

3.2.4. Effect of Na$_{10}$[α-SiW$_9$O$_{34}$] concentration. In order to achieve the best performance, we investigated the effect of
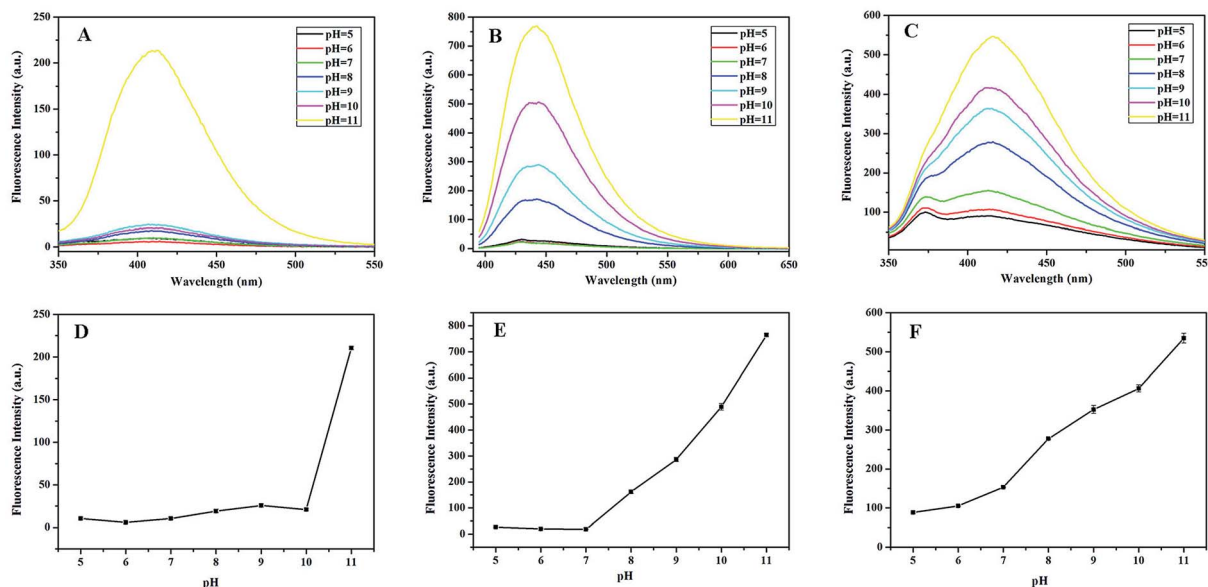

Fig. 3 The effects of pH on the fluorescence intensities of the (A and D) BA–Na$_{10}$[α-SiW$_9$O$_{34}$]–H$_2$O$_2$ system, (B and E) TH–Na$_{10}$[α-SiW$_9$O$_{34}$]–H$_2$O$_2$ system and (C and F) HPPA–Na$_{10}$[α-SiW$_9$O$_{34}$]–H$_2$O$_2$ system. Reaction conditions: 8 mmol L^{-1} Na$_{10}$[α-SiW$_9$O$_{34}$]; 100 mmol L^{-1} H$_2$O$_2$; 5 mmol L^{-1} BA; 20 mmol L^{-1} TH; 80 mmol L^{-1} HPPA; temperature, 25 °C.
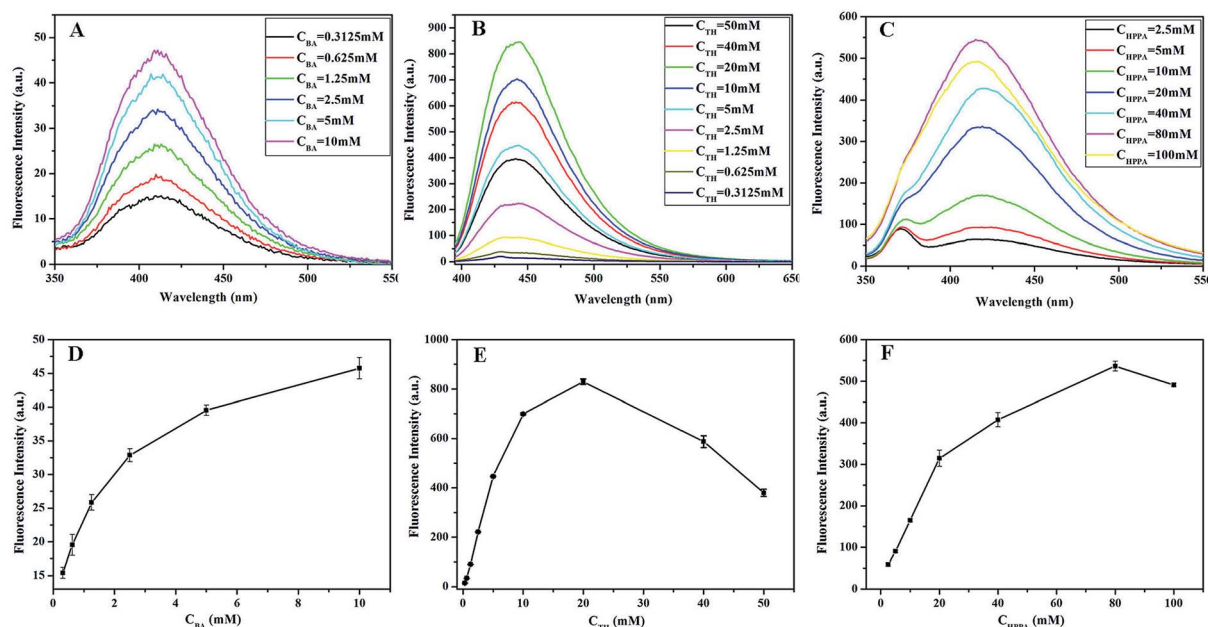
Fig. 4   The effects of different substrate concentrations on the fluorescence intensities of the (A and D) BA−Na$_{10}$[α-SiW$_9$O$_{34}$]−H$_2$O$_2$ system, (B and E) TH−Na$_{10}$[α-SiW$_9$O$_{34}$]−H$_2$O$_2$ system, and (C and F) HPPA−Na$_{10}$[α-SiW$_9$O$_{34}$]−H$_2$O$_2$ system. Reaction conditions: 8 mmol L^{-1} Na$_{10}$[α-SiW$_9$O$_{34}$]; 100 mmol L^{-1} H$_2$O$_2$; pH, 11.0; temperature, 25 °C.

Na$_{10}$[α-SiW$_9$O$_{34}$] concentrations (0.5–12 mM) on the fluorescence intensities of BA, TH and HPPA in the presence of H$_2$O$_2$. As shown in Fig. 5A and B, the fluorescence intensities all increased quickly with an increase in Na$_{10}$[α-SiW$_9$O$_{34}$] concentrations up to 8 mM, and then moderately slowly increased beyond 8 mM of Na$_{10}$[α-SiW$_9$O$_{34}$] in the BA and TH systems.

Whereas, in the HPPA−Na$_{10}$[α-SiW$_9$O$_{34}$]−H$_2$O$_2$ system, the fluorescence intensity first increased and then decreased, as shown in Fig. 5C. As shown in Fig. 5, when the concentration of Na$_{10}$[α-SiW$_9$O$_{34}$] reached 8 mM, the effect of Na$_{10}$[α-SiW$_9$O$_{34}$] on the fluorescence intensity in different substrate−Na$_{10}$[α-SiW$_9$O$_{34}$]−H$_2$O$_2$ systems achieved the best activity. Thus, aiming to obtain
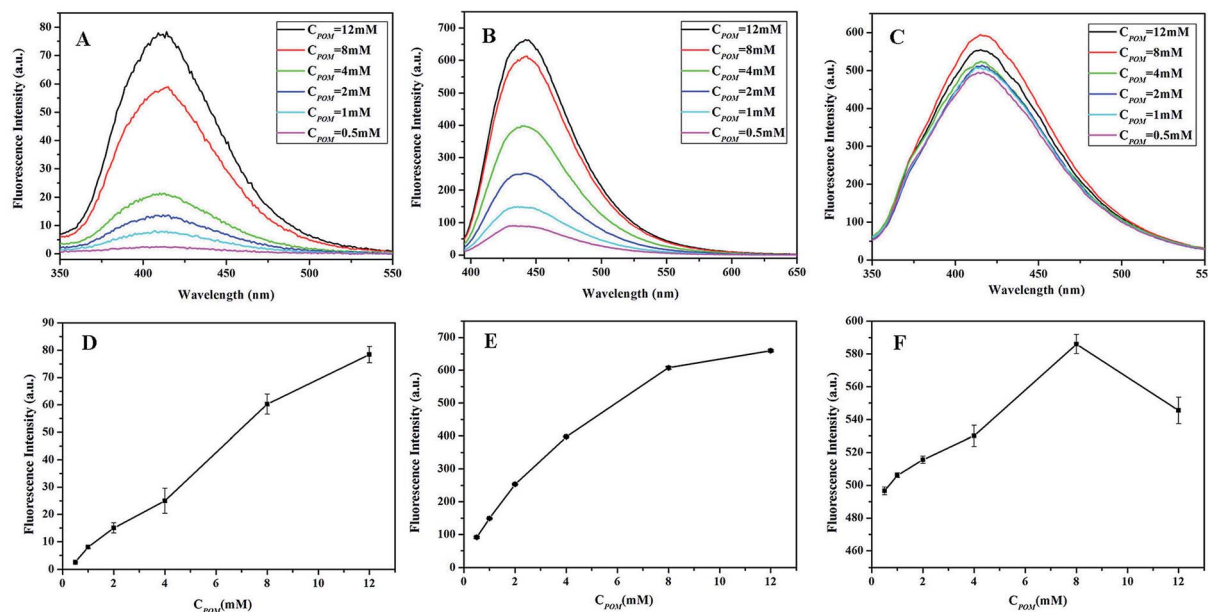
Fig. 5   The effects of Na$_{10}$[α-SiW$_9$O$_{34}$] concentrations on the fluorescence intensities of the (A and D) BA−Na$_{10}$[α-SiW$_9$O$_{34}$]−H$_2$O$_2$ system, (B and E) TH−Na$_{10}$[α-SiW$_9$O$_{34}$]−H$_2$O$_2$ system and (C and F) HPPA−Na$_{10}$[α-SiW$_9$O$_{34}$]−H$_2$O$_2$ system. Reaction conditions: 100 mmol L^{-1} H$_2$O$_2$; 5 mmol L^{-1} BA; 20 mmol L^{-1} TH; 80 mmol L^{-1} HPPA; pH, 11.0; temperature, 25 °C.

the best catalytic activity of $Na_{10}[\alpha\text{-}SiW_9O_{34}]$ and low economic cost, 8 mM $Na_{10}[\alpha\text{-}SiW_9O_{34}]$ was selected as the optimal concentration.
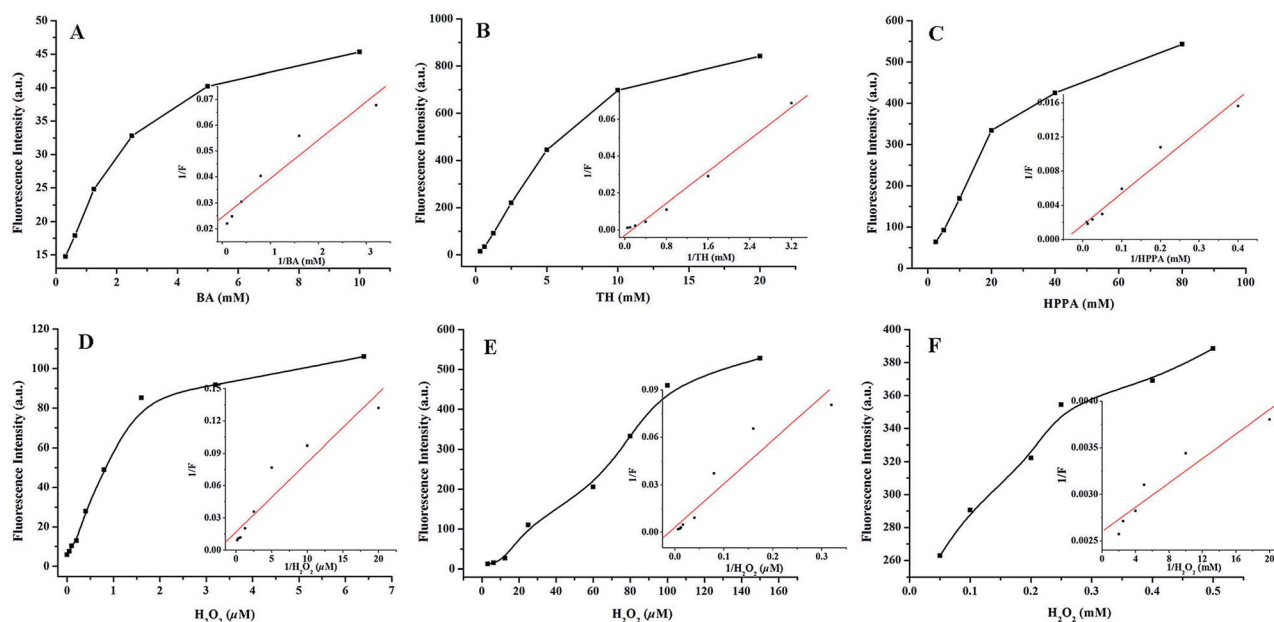
3.3. Steady-state kinetic assay

For a further understanding of the influence of different substrates on the catalytic mechanism of $Na_{10}[\alpha\text{-}SiW_9O_{34}]$ in the presence of H_2O_2, steady-state kinetic assays for different substrates were determined in detail. As shown in Fig. 6, the typical Michaelis–Menten curve was obtained for $Na_{10}[\alpha\text{-}SiW_9O_{34}]$ in the presence of H_2O_2. Michaelis–Menten constant (K_M) and maximum initial velocity (V_{max}) were counted from the Michaelis–Menten curve using a Lineweaver–Burk plot. The kinetic parameters of BA, TH, and HPPA are given in Table 1. The K_M of $Na_{10}[\alpha\text{-}SiW_9O_{34}]$ with BA, TH and HPPA as substrates were 6.03×10^{-4}, 7.95×10^{-3} and 2.12×10^{-2} M, respectively. The V_{max} of $Na_{10}[\alpha\text{-}SiW_9O_{34}]$ with BA, TH, and HPPA as substrates were 4.06×10^{-4}, 3.68×10^{-5} and 5.75×10^{-5} M s^{-1}, respectively. The K_M of BA, TH, and HPPA using $Na_{10}[\alpha\text{-}SiW_9O_{34}]$ as a catalyst with H_2O_2 as the substrate were 3.75×10^{-7}, 8.31×10^{-5} and 2.51×10^{-2} M, respectively. The V_{max} of BA, TH, and HPPA using $Na_{10}[\alpha\text{-}SiW_9O_{34}]$ as a catalyst with H_2O_2 as the substrate were 5.82×10^{-4}, 3.02×10^{-5} and 3.85×10^{-5} M s^{-1}, respectively. The K_M value of $Na_{10}[\alpha\text{-}SiW_9O_{34}]$ with BA as the substrate was apparently lower than those values in the TH and HPPA systems. This indicated that BA has a higher affinity to $Na_{10}[\alpha\text{-}SiW_9O_{34}]$ in comparison with TH and HPPA. The apparent K_M value of BA with H_2O_2 as the substrate was apparently lower than those values in TH and HPPA. It was clear that BA has a higher affinity for H_2O_2 compared with those of TH and HPPA.

Table 1 Comparison of the K_M and V_{max} values of BA, TH and HPPA using $Na_{10}[\alpha\text{-}SiW_9O_{34}]$ as a catalyst

Enzyme	Substrate	K_M (M)	V_{max} (M S^{-1})
$Na_{10}[\alpha\text{-}SiW_9O_{34}]$	BA	6.03×10^{-4}	4.06×10^{-4}
$Na_{10}[\alpha\text{-}SiW_9O_{34}]$	H_2O_2	3.75×10^{-7}	5.82×10^{-4}
$Na_{10}[\alpha\text{-}SiW_9O_{34}]$	TH	7.95×10^{-3}	3.68×10^{-5}
$Na_{10}[\alpha\text{-}SiW_9O_{34}]$	H_2O_2	8.31×10^{-5}	3.02×10^{-5}
$Na_{10}[\alpha\text{-}SiW_9O_{34}]$	HPPA	2.12×10^{-2}	5.75×10^{-5}
$Na_{10}[\alpha\text{-}SiW_9O_{34}]$	H_2O_2	2.51×10^{-2}	3.85×10^{-5}

3.4. Calibration curve for H_2O_2 detection

Under the optimized reaction conditions, the relationships between the fluorescence intensities and H_2O_2 concentrations in the BA–$Na_{10}[\alpha\text{-}SiW_9O_{34}]$–$H_2O_2$, TH–$Na_{10}[\alpha\text{-}SiW_9O_{34}]$–$H_2O_2$ and HPPA–$Na_{10}[\alpha\text{-}SiW_9O_{34}]$–$H_2O_2$ systems were investigated. As shown in Fig. 7D, the fluorescence intensity of BA–$Na_{10}[\alpha\text{-}SiW_9O_{34}]$–$H_2O_2$ increased linearly with increasing concentrations of H_2O_2. The linear regression equation was as follows: $Y = 4.45 + 5.22 \times 10^7 \times C_{H_2O_2}$ with a correlation coefficient of 0.97403; the linear range was from 1×10^{-8} to 1.6×10^{-6} M. The lower limit of detection (3σ, LOD) of $Na_{10}[\alpha\text{-}SiW_9O_{34}]$ for H_2O_2 was found to be 6.7×10^{-9} M. As shown in Fig. 7E, the fluorescence intensity of TH–$Na_{10}[\alpha\text{-}SiW_9O_{34}]$–$H_2O_2$ increased linearly with increasing concentrations of H_2O_2. The linear regression equation was as follows: $Y = 8.41 + 4.35 \times 10^6 \times C_{H_2O_2}$ with a correlation coefficient of 0.99049; the linear range was from 1.6×10^{-6} to 1×10^{-4} M. The LOD of the $Na_{10}[\alpha\text{-}SiW_9O_{34}]$ for H_2O_2 was found to be 2.2×10^{-7} M. Moreover, as shown in Fig. 7F, the fluorescence intensity of HPPA–$Na_{10}[\alpha\text{-}SiW_9O_{34}]$–$H_2O_2$ increased linearly with increasing

Fig. 6 The steady-state kinetic assays and catalytic mechanisms of $Na_{10}[\alpha\text{-}SiW_9O_{34}]$ as a catalyst in different substrates: (A and D) BA–$Na_{10}[\alpha\text{-}SiW_9O_{34}]$–$H_2O_2$ system, (B and E) TH–$Na_{10}[\alpha\text{-}SiW_9O_{34}]$–$H_2O_2$ system and (C and F) HPPA–$Na_{10}[\alpha\text{-}SiW_9O_{34}]$–$H_2O_2$ system. Reaction conditions: 8 mmol L^{-1} $Na_{10}[\alpha\text{-}SiW_9O_{34}]$; pH, 11.0; temperature, 25 °C; incubation time, 10 min.

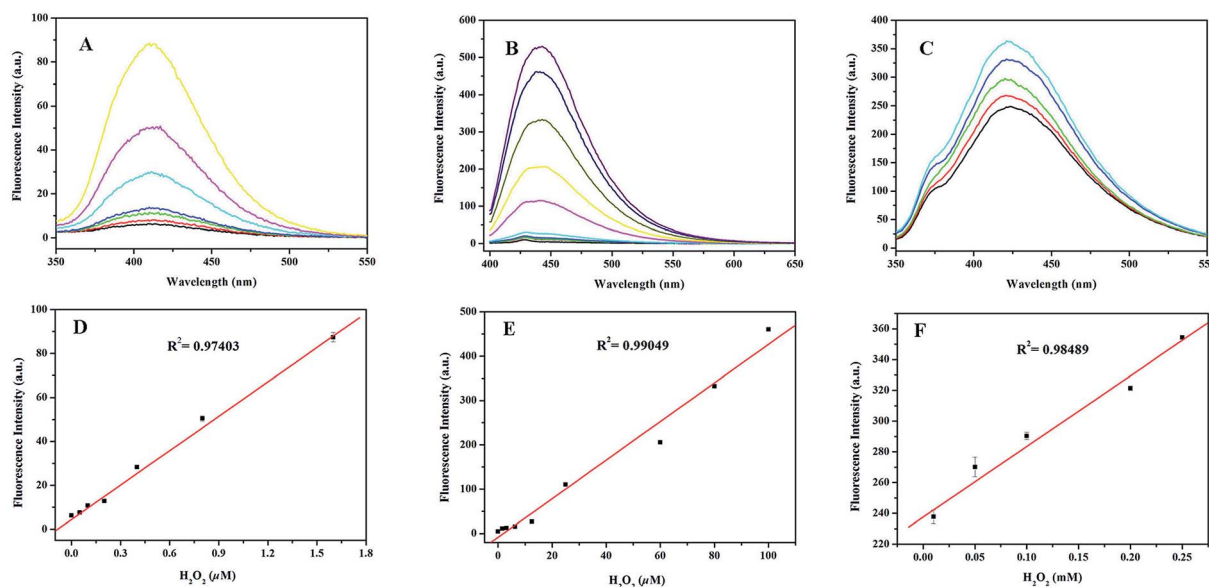**Fig. 7** Linear calibration plots for H_2O_2: (A and D) BA–$Na_{10}[\alpha$-$SiW_9O_{34}]$–H_2O_2 system, (B and E) TH–$Na_{10}[\alpha$-$SiW_9O_{34}]$–H_2O_2 system, and (C and F) HPPA–$Na_{10}[\alpha$-$SiW_9O_{34}]$–H_2O_2 system. Reaction conditions: 8 mmol L^{-1} $Na_{10}[\alpha$-$SiW_9O_{34}]$; 5 mmol L^{-1} BA; 20 mmol L^{-1} TH; 80 mmol L^{-1} HPPA; pH, 11.0; temperature, 25 °C; incubation time, 10 min.

concentration of H_2O_2. The linear regression equation was as follows: $Y = 237.55 + 4.60 \times 10^5 \times C_{H_2O_2}$ with a correlation coefficient of 0.98489; the linear range was from 1×10^{-5} to 2.5×10^{-4} M. The LOD of $Na_{10}[\alpha$-$SiW_9O_{34}]$ for H_2O_2 was found to be 9.6×10^{-6} M. Comparing these systems for the determination of H_2O_2, as shown in Table 2, the proposed method is superior in its low detection limit.

3.5. Interference study

For further evaluating the detection selectivity of BA–$Na_{10}[\alpha$-$SiW_9O_{34}]$, TH–$Na_{10}[\alpha$-$SiW_9O_{34}]$ and HPPA–$Na_{10}[\alpha$-$SiW_9O_{34}]$ systems for H_2O_2 determination, investigations were carried out at H_2O_2 concentrations of 5×10^{-7}, 5×10^{-5} and 5×10^{-4} mol L^{-1} with various coexisting substrates added. The results for BA–$Na_{10}[\alpha$-$SiW_9O_{34}]$–H_2O_2 are shown in Table 3. And the results for TH–$Na_{10}[\alpha$-$SiW_9O_{34}]$–H_2O_2 and HPPA–$Na_{10}[\alpha$-$SiW_9O_{34}]$–H_2O_2 systems are shown in Tables S1 and S2.† It can

be observed that none of the substances shows any obvious interference. Thus, these proposed fluorometric methods display a high selectivity for the determination of H_2O_2.

3.6. Determination of H_2O_2 in water samples

In order to evaluate the feasibility of the proposed methods, we tested the content of H_2O_2 in water samples under the optimum conditions. Each sample was analyzed at the same time with all the methods in order to avoid any possible differences caused by degradation of the analyte in the sample. The results of the BA–$Na_{10}[\alpha$-$SiW_9O_{34}]$–H_2O_2 system are presented in Table 4, where it can be seen that the data for recoveries was between 99.73% and 113.06%. The RSD of detection ranged from 2.57% to 4.66%. The results of the TH–$Na_{10}[\alpha$-$SiW_9O_{34}]$–H_2O_2 system are shown in Table S3.† For each sample, three parallel experiments were conducted, and the RSD of detection ranged from 0.82% to 4.06%. The recoveries of the samples were between

Table 2 Comparison of different fluorescent systems for the detection of H_2O_2

System	Linear range[a]	Detection limit[a]	Reference
BA–BFO MNPs system	2.0×10^{-8} to 2.0×10^{-5}	4.5×10^{-9}	13
BA–·OH	1.1×10^{-5} to 1.1×10^{-3}	1.0×10^{-6}	44
CuO NPs/HPPA	5.0×10^{-5} to 4.0×10^{-4}	8.1×10^{-7}	41
Hb–H_2O_2–thiamine	1.0×10^{-7} to 8.0×10^{-5}	2.6×10^{-8}	40
HRP–Cy.7.Cl	1.8×10^{-7} to 7.2×10^{-6}	5.6×10^{-8}	4
HBcAb–HRP–CdTe QDs	1.0×10^{-7} to 1.5×10^{-4}	6.9×10^{-8}	45
CdTe–$Na_{10}[\alpha$-$SiW_9O_{34}]$–H_2O_2	7.8×10^{-9} to 2.5×10^{-7}	3.8×10^{-9}	39
BA–$Na_{10}[\alpha$-$SiW_9O_{34}]$–H_2O_2	1.0×10^{-8} to 1.6×10^{-6}	6.7×10^{-9}	This work
TH–$Na_{10}[\alpha$-$SiW_9O_{34}]$–H_2O_2	1.6×10^{-6} to 1.0×10^{-4}	2.2×10^{-7}	This work
HPPA–$Na_{10}[\alpha$-$SiW_9O_{34}]$–H_2O_2	1.0×10^{-5} to 2.5×10^{-4}	9.6×10^{-6}	This work

[a] mol L^{-1}.

Table 3 The interference study for the determination of H_2O_2 (5×10^{-7} mol L^{-1}) by the proposed method

Coexisting substance	Content (mol L^{-1})	$\Delta I^a/I$ (%)
Na^+	5×10^{-3}	1.25
K^+	5×10^{-3}	−1.96
NH_4^+	5×10^{-3}	−1.26
SO_4^{2-}	2×10^{-3}	−2.80
Mn^{2+}	2×10^{-3}	2.90
Cl^-	2×10^{-3}	2.38
CO_3^{2-}	2×10^{-3}	−7.50
Glucose	2×10^{-3}	−2.47
Citric acid	2×10^{-3}	1.77

^{a} $\Delta I = I_0 - I$, where I_0 and I are the fluorescence intensities of the BA–$Na_{10}[\alpha\text{-}SiW_9O_{34}]$–$H_2O_2$ system in the absence and presence of interfering species.

Table 4 Results of the analyses of H_2O_2 in water samples, when the substrate was BA

Sample	Added (μM)	Detected (μM)	Recovery (%)	RSD (n = 3, %)
1	0.4	0.455 ± 0.0212	113.06	4.66
2	0.8	0.878 ± 0.0239	109.46	2.73
3	1.6	1.599 ± 0.0411	99.73	2.57

95.20% and 104.22%. The results for the HPPA–$Na_{10}[\alpha\text{-}SiW_9O_{34}]$–$H_2O_2$ system are listed in Table S4.† From Table S4,† the recoveries of H_2O_2 were found to range from 95.28% to 128.76%, and the RSD of detection ranges from 1.08% to 2.75%. The results demonstrated that these proposed methods for H_2O_2 determination were acceptable and suitable.

4. Conclusions

In summary, we established for the first time new fluorometric enhancement methods for the detection of hydrogen peroxide on the basis of the catalytic activation of $Na_{10}[\alpha\text{-}SiW_9O_{34}]$ in alkaline H_2O_2 bleaching systems. H_2O_2 can be decomposed into ·OH radicals in the presence of $Na_{10}[\alpha\text{-}SiW_9O_{34}]$, which could turn non-fluorescent substrates into a strongly fluorescent product. Under the optimal reaction conditions, linear correlation was established between fluorescence intensity and the concentration of H_2O_2. These methods will help in monitoring H_2O_2 doses and its related products, such as hydroxyl radicals, under complex practical conditions, but also in the further detection of the meaningful fluorogenic substrates, BA, TH and HPPA.

Conflicts of interest

There are no conflicts to declare.

Acknowledgements

References

1 Y. Tao, E. G. Ju, J. S. Ren and X. G. Qu, *Chem. Commun.*, 2014, **50**, 3030–3032.

2 H. Q. Chen, H. P. Yu, Y. Y. Zhou and L. Wang, *Spectrochim. Acta, Part A*, 2007, **67**, 683–686.

3 X. S. Chai, Q. X. Hou, Q. Luo and J. Y. Zhu, *Anal. Chim. Acta*, 2004, **507**, 281–284.

4 B. Tang, L. Zhang and K. H. Xu, *Talanta*, 2006, **68**, 876–882.

5 B. Tang, L. Zhang and Y. Geng, *Talanta*, 2005, **65**, 769–775.

6 G. C. Van de Bittner, E. A. Dubikovskaya, C. R. Bertozzi and C. J. Chang, *Proc. Natl. Acad. Sci. U. S. A.*, 2010, **107**, 21316–21321.

7 P. A. Tanner and A. Y. S. Wong, *Anal. Chim. Acta*, 1998, **370**, 279–287.

8 B. Tang, Y. Wang, Y. Sun and H. X. Shen, *Spectrochim. Acta, Part A*, 2002, **58**, 141–148.

9 J. M. Lin and M. Yamada, *Anal. Chem.*, 1999, **71**, 1760–1766.

10 H. F. Yue, X. Bu, M. H. Huang, J. Young and T. Raglione, *Int. J. Pharm.*, 2009, **375**, 33–40.

11 L. S. Jahnke, *Anal. Biochem.*, 1999, **269**, 273–277.

12 K. Hensley, K. S. Williamson, M. L. Maidt, S. P. Gabbita, P. Grammas and R. A. Floyd, *HRC J. High Resolut. Chromatogr.*, 1999, **22**, 429–437.

13 W. Luo, Y. S. Li, J. Yuan, L. H. Zhu, Z. D. Liu, H. Q. Tang and S. S. Liu, *Talanta*, 2010, **81**, 901–907.

14 X. Chen, D. Li, H. Yang, Q. Zhu, H. Zheng and J. Xu, *Anal. Chim. Acta*, 2001, **434**, 51–58.

15 E. Kuah, S. Toh, J. Yee, Q. Ma and Z. Q. Gao, *Chem.–Eur. J.*, 2016, **22**, 8404–8430.

16 R. Breslow and L. E. Overman, *J. Am. Chem. Soc.*, 1970, **92**, 1075–1077.

17 Y. Aiba, J. Sumaoka and M. Komiyama, *Chem. Soc. Rev.*, 2011, **40**, 5657–5668.

18 R. P. Bonarlaw and J. K. M. Sanders, *J. Am. Chem. Soc.*, 1995, **117**, 259–271.

19 G. P. Royer and I. M. Klotz, *J. Am. Chem. Soc.*, 1969, **91**, 5885–5886.

20 X. Zhang, H. P. Xu, Z. Y. Dong, Y. P. Wang, J. Q. Liu and J. C. Shen, *J. Am. Chem. Soc.*, 2004, **126**, 10556–10557.

21 D. J. Cram and J. M. Cram, *Science*, 1974, **183**, 803–809.

22 J. M. Lehn and C. Sirlin, *J. Chem. Soc., Chem. Commun.*, 1978, 949–951.

23 Z. Y. Dong, Y. G. Wang, Y. Z. Yin and J. Q. Liu, *Curr. Opin. Colloid Interface Sci.*, 2011, **16**, 451–458.

24 G. Wulff and A. Sarhan, *Angew. Chem., Int. Ed. Engl.*, 1972, **11**, 341–342.

25 T. Takagish and I. M. Klotz, *Biopolymers*, 1972, **11**, 483–491.

26 T. Pan and O. C. Uhlenbeck, *Biochemistry*, 1992, **31**, 3887–3895.

27 R. R. Breaker and G. F. Joyce, *Chem. Biol.*, 1994, **1**, 223–229.

28 S. J. Pollack, J. W. Jacobs and P. G. Schultz, *Science*, 1986, **234**, 1570–1573.

29 D. L. Long, R. Tsunashima and L. Cronin, *Angew. Chem., Int. Ed.*, 2010, **49**, 1736–1758.

30 M. T. Pope and A. Müller, *Angew. Chem., Int. Ed.*, 1991, **30**, 34–48.

31 J. J. Wang, X. G. Mi, H. Y. Guan, X. H. Wang and Y. Wu, *Chem. Commun.*, 2011, **47**, 2940–2942.

32 S. Liu, J. Q. Tian, L. Wang, Y. W. Zhang, Y. L. Luo, H. Y. Li, A. M. Asiri, A. O. Al-Youbi and X. P. Sun, *Chempluschem*, 2012, **77**, 541–544.

33 J. J. Wang, D. X. Han, X. H. Wang, B. Qi and M. S. Zhao, *Biosens. Bioelectron.*, 2012, **36**, 18–21.

34 D. Li, H. Y. Han, Y. H. Wang, X. Wang, Y. G. Li and E. B. Wang, *Eur. J. Inorg. Chem.*, 2013, 1926–1934.

35 C. L. Sun, X. L. Chen, J. Xu, M. J. Wei, J. J. Wang, X. G. Mi, X. H. Wang, Y. Wu and Y. Liu, *J. Mater. Chem. A.*, 2013, **1**, 4699–4705.

36 Z. Sun, H. Z. Bie, M. J. Wei, J. J. Wang, X. G. Mi, X. H. Wang and Y. Wu, *Chin. Chem. Lett.*, 2013, **24**, 76–78.

37 Y. Ji, J. Xu, X. L. Chen, L. Han, X. H. Wang, F. Chai and M. S. Zhao, *Sens. Actuators, B*, 2015, **208**, 497–504.

38 Z. Ma, Y. F. Qiu, H. H. Yang, Y. M. Huang, J. J. Liu, Y. Lu, C. Zhang and P. A. Hu, *ACS Appl. Mater. Interfaces*, 2015, **7**, 22036–22045.

39 R. Tian, B. Y. Zhang, M. M. Zhao, Q. Ma and Y. F. Qi, *Talanta*, 2018, **188**, 332–338.

40 C. L. Xu and Z. J. Zhang, *Anal. Sci.*, 2001, **17**, 1449–1451.

41 H. H. Deng, X. Q. Zheng, Y. Y. Wu, X. Q. Shi, X. L. Lin, X. H. Xia, H. P. Peng, W. Chen and G. L. Hong, *Analyst*, 2017, **142**, 3986–3992.

42 A. Téazéa, G. Hervéa, R. G. Finke and D. K. Lyon, *Inorg. Synth.*, 1990, **27**, 85–96.

43 K. Zaitsu and Y. Ohkura, *Anal. Biochem.*, 1980, **109**, 109–113.

44 F. Si, X. Zhang and K. L. Yan, *RSC Adv.*, 2014, **4**, 5860–5866.

45 T. T. Gong, J. F. Liu, Y. W. Wu, Y. Xiao, X. H. Wang and S. Q. Yuan, *Biosens. Bioelectron.*, 2017, **92**, 16–20.